



Supplement of

Multivariate calibration can increase simulated discharge uncertainty and model equifinality

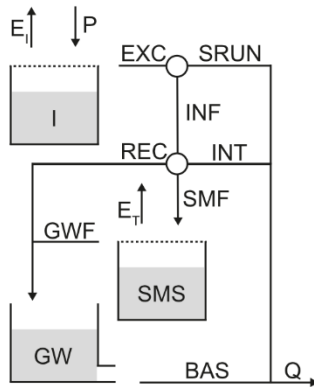
Sandra Pool et al.

Correspondence to: Sandra Pool (sandra.pool@eawag.ch)

The copyright of individual parts of the supplement might differ from the article licence.

The SIMHYD model

Model structure:



Model stores and fluxes:

P: precipitation	= input data
ET_0 : potential evaporation	= input data
I: current interception storage	$= dl/dt = P - E_I - EXC$
E_I : evaporation from interception	$= \{ET_0 \text{ if } I > 0, 0 \text{ otherwise}\}$
EXC: excess precipitation	$= \{P \text{ if } I = INSC, 0 \text{ otherwise}\}$
SMS: current soil moisture storage	$= dSMS/dt = SMF - E_T - GWF$
INF: total infiltration	$= \min(COEFF \times \exp(-SQ \times SMS / SMS C), EXC)$
SMF: flow into SMS	$= INF - INT - REC$
SRUN: infiltration excess overland flow	$= EXC - INF$
INT: interflow and saturation excess overland flow	$= SUB \times SMS / SMS C \times INF$
REC: preferential recharge	$= CRAK \times SMS / SMS C \times (INF - INT)$
E_T : evaporation from soil	$= \min(10 \times SMS / SMS C, PET)$
GWF: flow into GW	$= \{SMF \text{ if } SMF = SMS C, 0 \text{ otherwise}\}$
GW: groundwater store	$= dGW/dt = REC + GWF - BAS$
BAS: baseflow	$= K \times GW$
Q: streamflow	$= SRUN + INT + BASE$

Model parameters:

INSC : maximum interception store capacity [mm]
COEFF : maximum infiltration loss [mm/day]
SQ : infiltration loss exponent [-]
SMSC : maximum soil moisture store capacity [mm]
SUB : constant of proportionality in interflow equation [-]
CRAK : constant of proportionality in groundwater recharge equation [-]
K : baseflow linear recession parameter [1/day]

Figure S1. The SIMHYD model. The schematic of the model structure, and the definition of model stores, fluxes, and parameters are based on the Modular Assessment of Rainfall-Runoff Models Toolbox (MARRMoT) version 2.1 (Trotter et al., 2022).

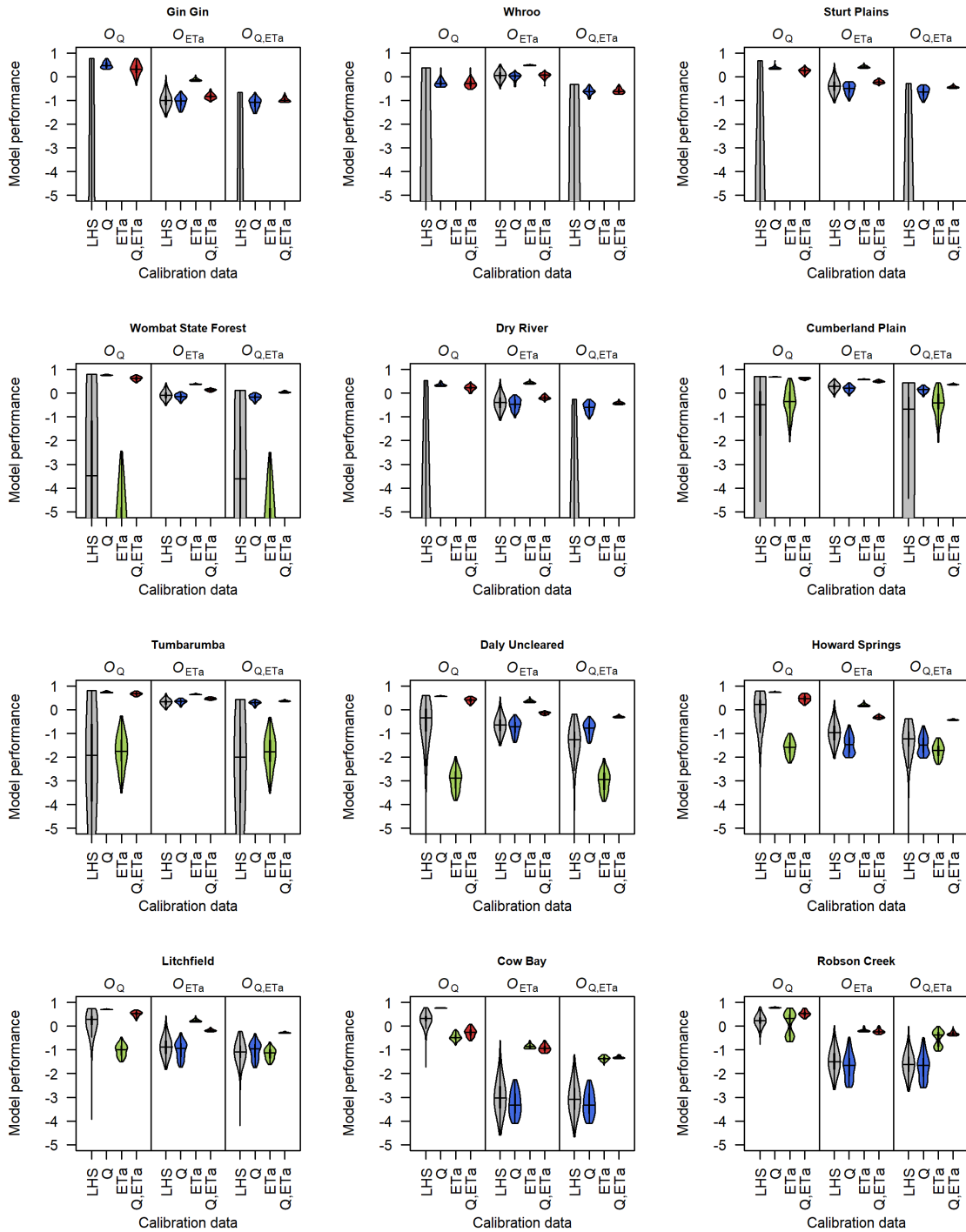


Figure S2. Model performance for discharge (O_Q), actual evapotranspiration (O_{ETa}), and discharge and actual evapotranspiration ($O_{Q,ETa}$). Performance is shown for all 100,000 randomly selected parameter values (LHS), and the 100 best performing parameter values selected using discharge (Q), actual evapotranspiration (ETa), and discharge and actual evapotranspiration (Q,ETa). Results are shown for the dataset using *remote sensing-based* actual evapotranspiration ($D_{ETa,RS}$).

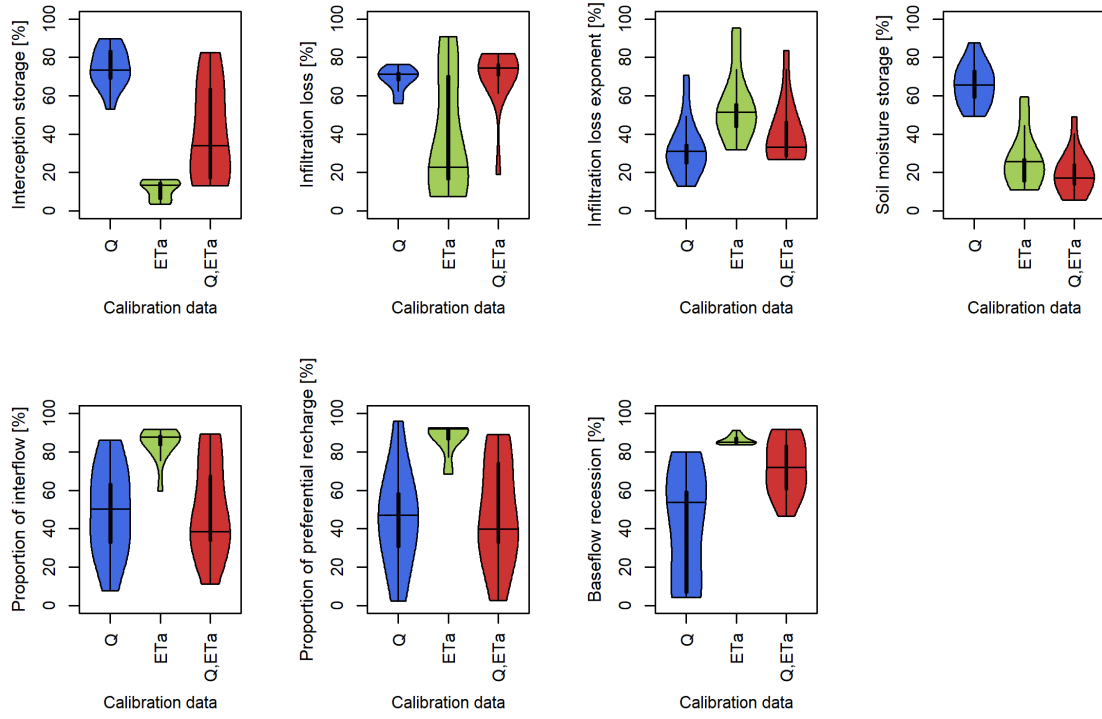


Figure S3. Ratio of the range of parameter values of the SIMHYD model for the twelve study catchments after calibration to the range of parameter values before calibration. The range after calibration is based on the 100 best performing parameter values selected using discharge (Q), actual evapotranspiration (ETa), and discharge and actual evapotranspiration (Q,ETa). The range of parameter values after calibration is calculated as the difference between the 10th and 90th quantile. The range before calibration is based on all 100,000 randomly selected parameter values. Results are shown for the dataset using *remote sensing-based* actual evapotranspiration ($D_{ETa,RS}$).

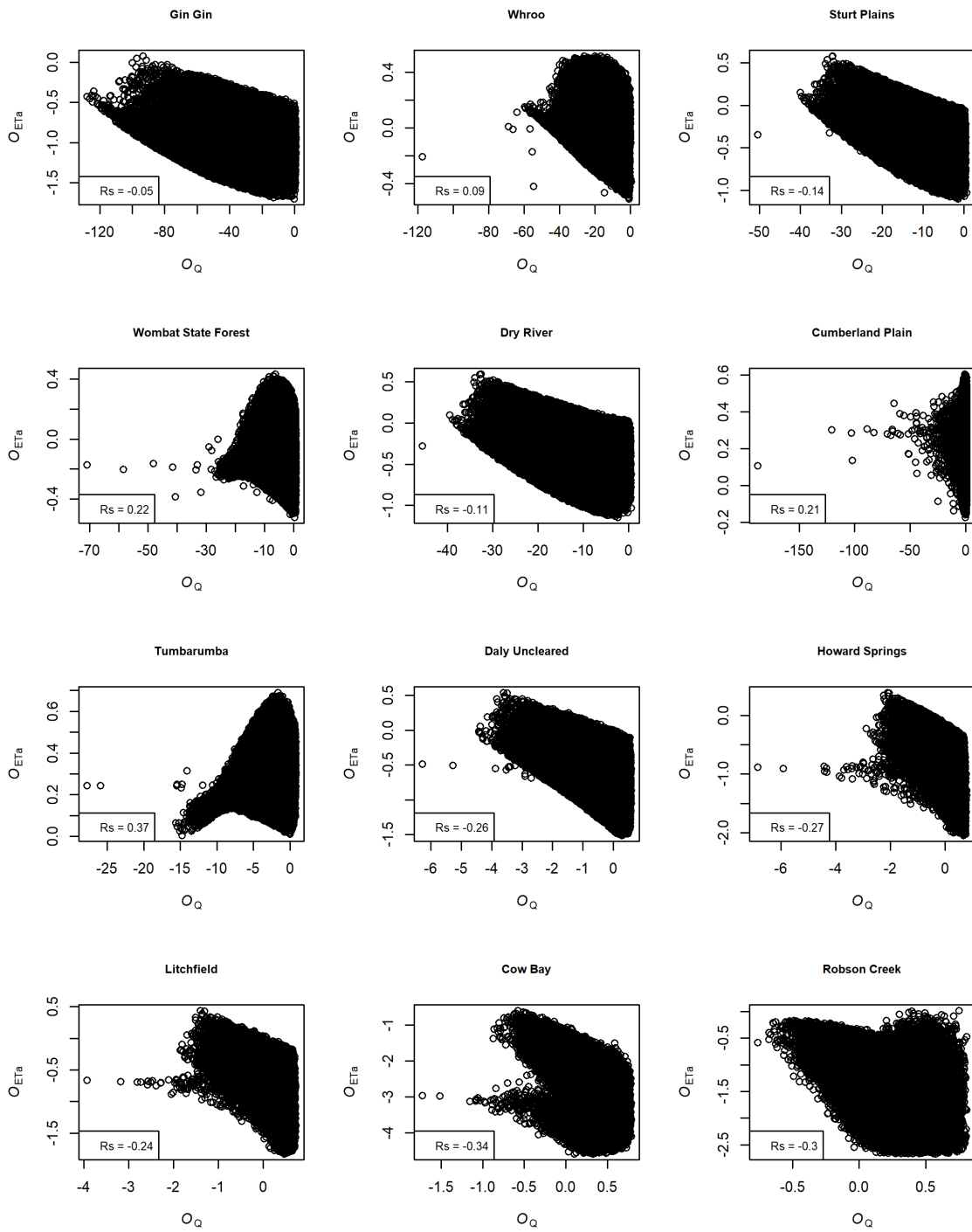


Figure S4. Correlation between model performance for discharge (O_Q) and actual evapotranspiration (O_{ETa}) for all 100,000 randomly selected parameter values. R_s values show the Spearman rank correlation coefficients between the two objective functions. Results are shown for the dataset using *remote sensing-based* actual evapotranspiration ($D_{ETa,RS}$).

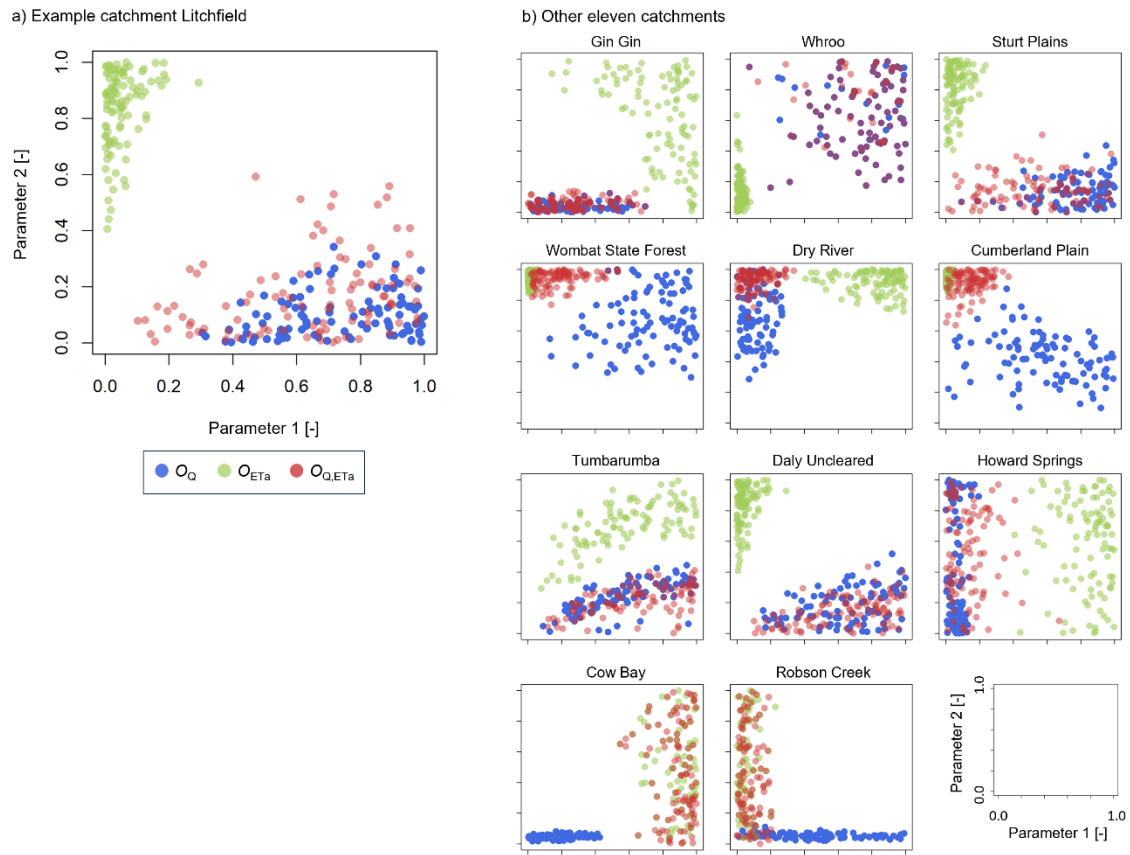


Figure S5. Parameter distribution when calibrating the model with discharge (O_Q), actual evapotranspiration (O_{ETa}), or discharge and actual evapotranspiration ($O_{Q,ETa}$). This figure is the same as Fig. 4 in the manuscript with the difference that results are shown for all three calibration cases: (a) Distribution of two parameters for the 100 best parameter sets in terms of O_Q , O_{ETa} , and $O_{Q,ETa}$ for the Litchfield catchment. In this example, parameter 1 is infiltration loss exponent [-] and parameter 2 is infiltration loss [mm d^{-1}]. (b) Same as in (a) but with an example for the other eleven catchments. Note that parameter 1 and parameter 2 represent different SIMHYD parameters in each case. Results are shown for the dataset using *remote sensing-based* actual evapotranspiration ($D_{ETa,RS}$).

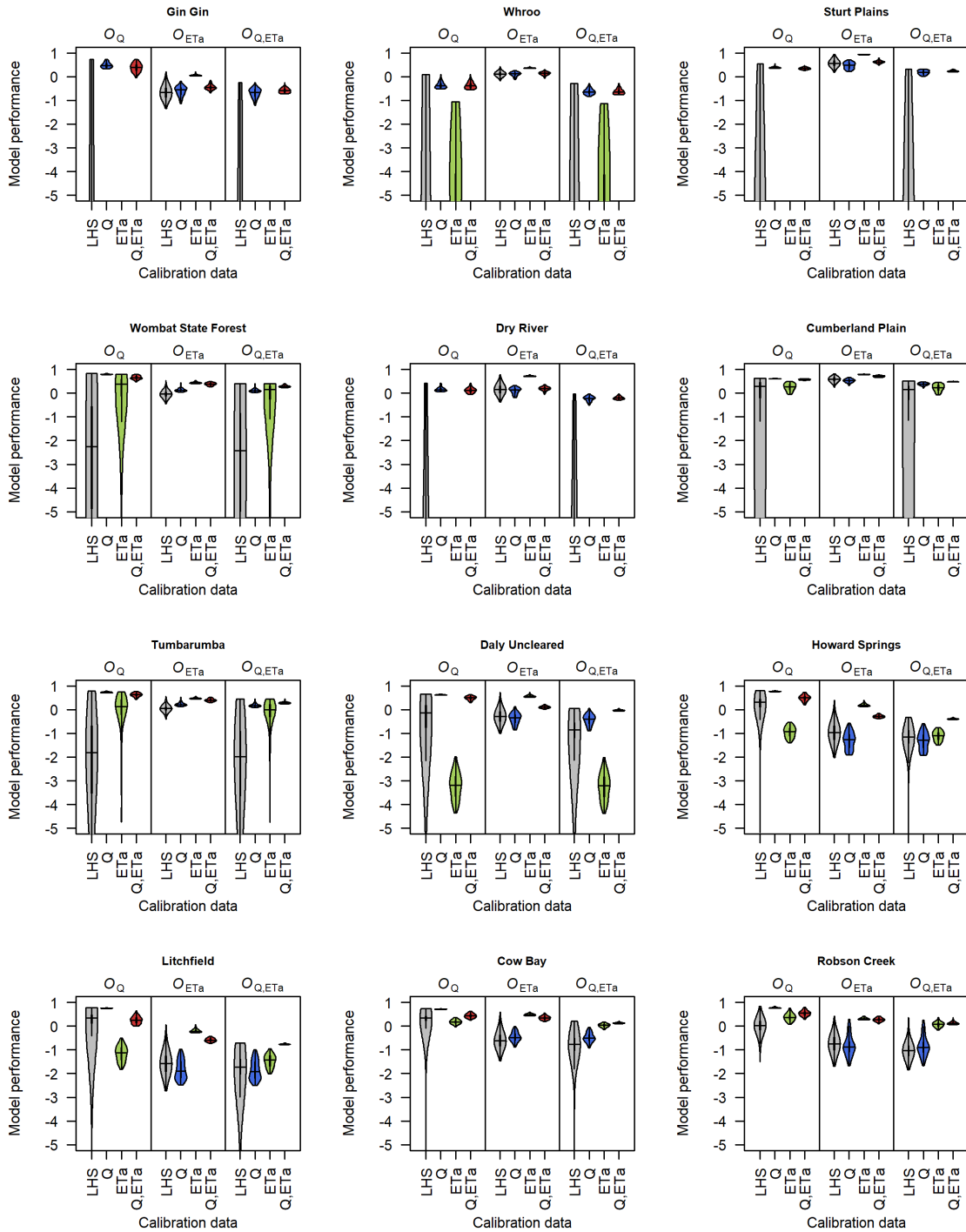


Figure S6. Repeat of Fig. S2 from the supporting information, but using *field-based* actual evapotranspiration ($D_{ETa,Field}$) rather than remotely sensed information. The figure shows model performance for discharge (O_Q), actual evapotranspiration (O_{ETa}), and discharge and actual evapotranspiration ($O_{Q,ETa}$). Performance is shown for all 100,000 randomly selected parameter values (LHS), and the 100 best performing parameter values selected using discharge (Q), actual evapotranspiration (ETa), and discharge and actual evapotranspiration (Q,ETa).

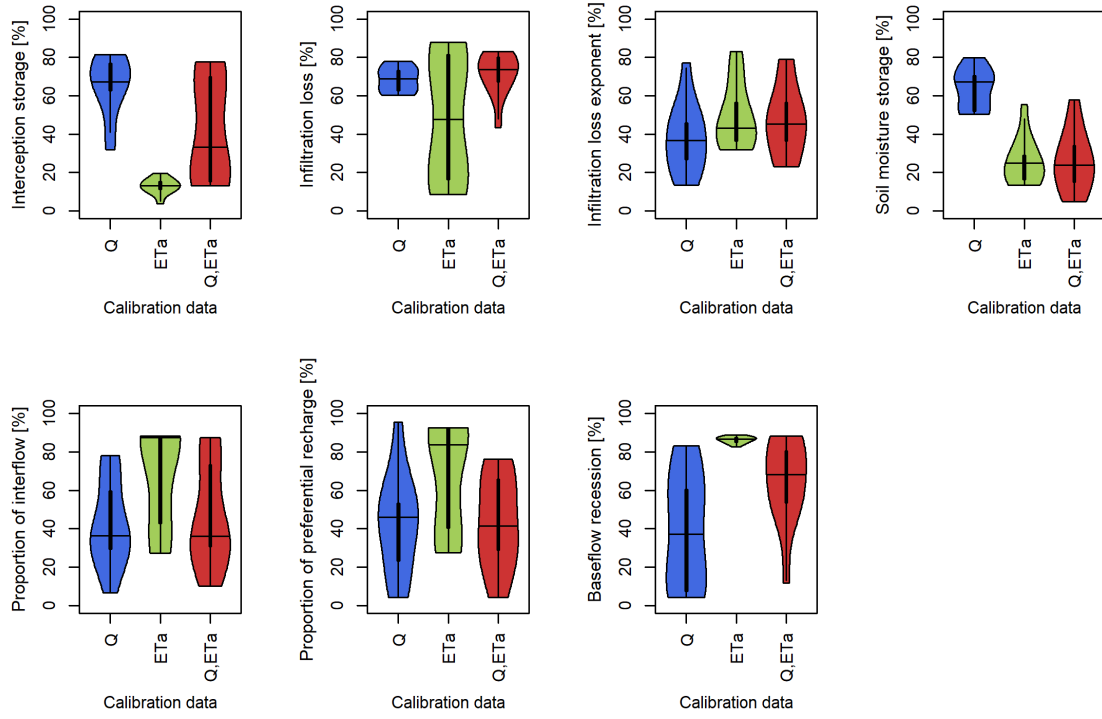


Figure S7. Repeat of Fig. S3 from the supporting information, but using *field-based* actual evapotranspiration ($D_{ETa,Field}$) rather than remotely sensed information. The figure shows the ratio of the range of parameter values of the SIMHYD model for the twelve study catchments after calibration to the range of parameter values before calibration. The range after calibration is based on the 100 best performing parameter values selected using discharge (Q), actual evapotranspiration (ETa), and discharge and actual evapotranspiration (Q,ETa). The range of parameter values after calibration is calculated as the difference between the 10th and 90th quantile. The range before calibration is based on all 100,000 randomly selected parameter values.

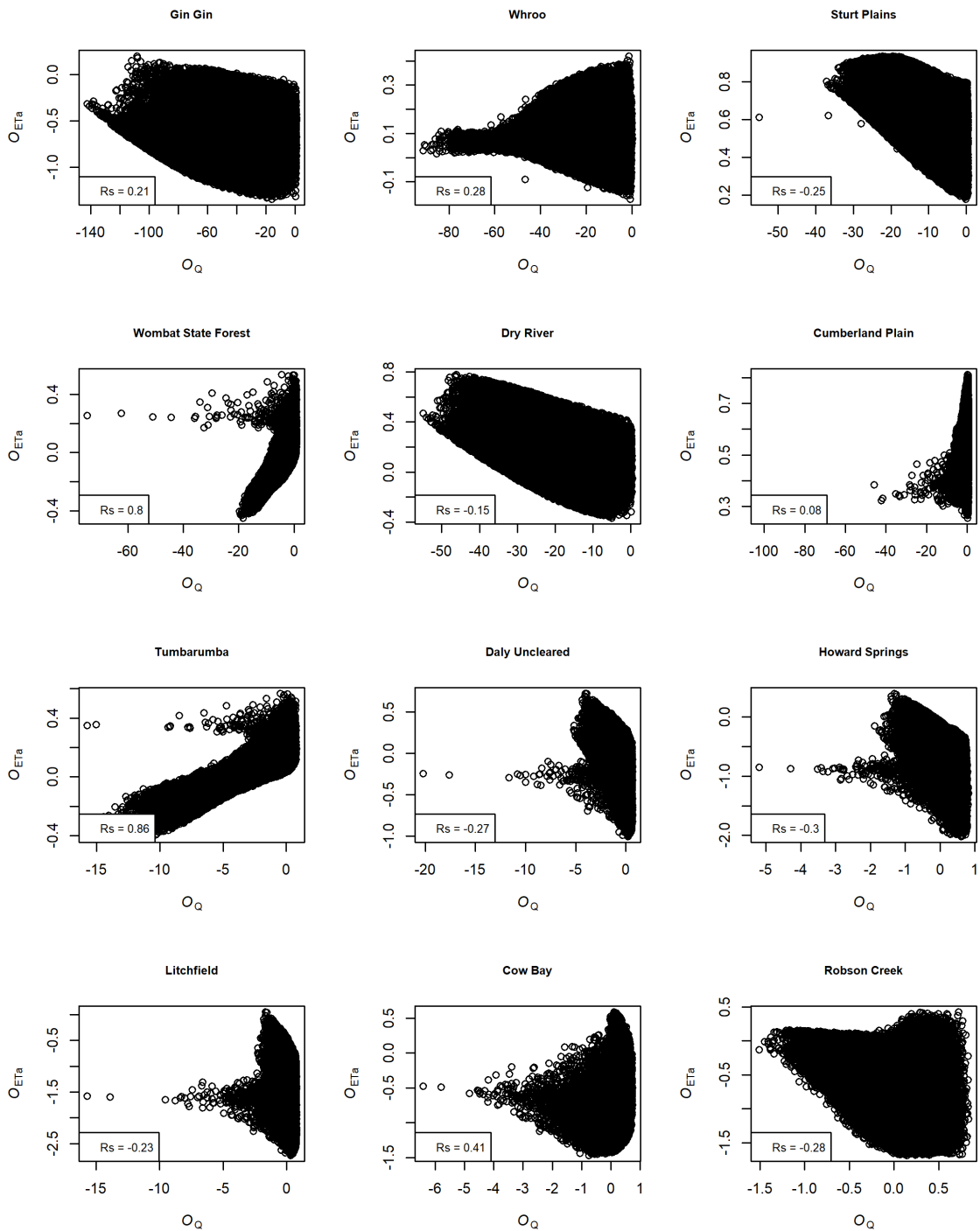


Figure S8. Repeat of Fig. S4 from the supporting information, but using *field-based* actual evapotranspiration ($O_{ETa,Field}$) rather than remotely sensed information. The figure shows the correlation between model performance for discharge (O_Q) and actual evapotranspiration (O_{ETa}) for all 100,000 randomly selected parameter values. R_s values show the Spearman rank correlation coefficients between the two objective functions.

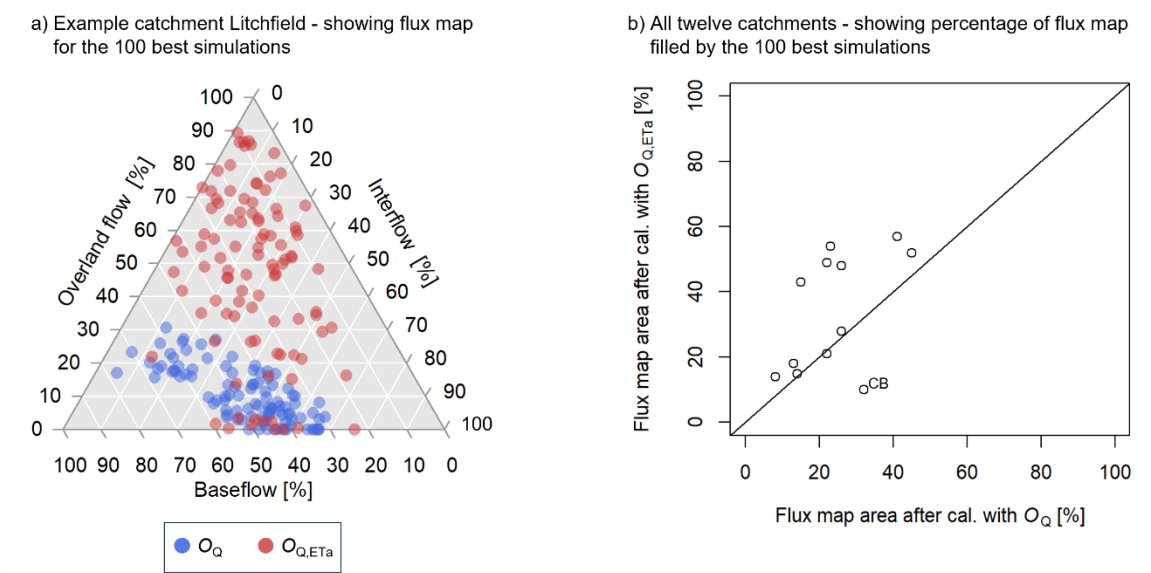


Figure S9. Repeat of Fig. 3 from the main paper, but using *field-based* actual evapotranspiration ($D_{ETa,Field}$) rather than remotely sensed information. The figure shows flux map uncertainty when calibrating the model with discharge (O_Q) or discharge and actual evapotranspiration ($O_{Q,ETa}$). (a) The flux map is shown for the 100 best parameter sets in terms of O_Q and $O_{Q,ETa}$ for the Litchfield catchment. (b) Percentage of flux map area covered by the ensemble of the 100 best parameter sets in terms of O_Q and $O_{Q,ETa}$. Values are shown for all twelve study catchments. The catchment Cow Bay (CB) is marked due to its different flux map area.

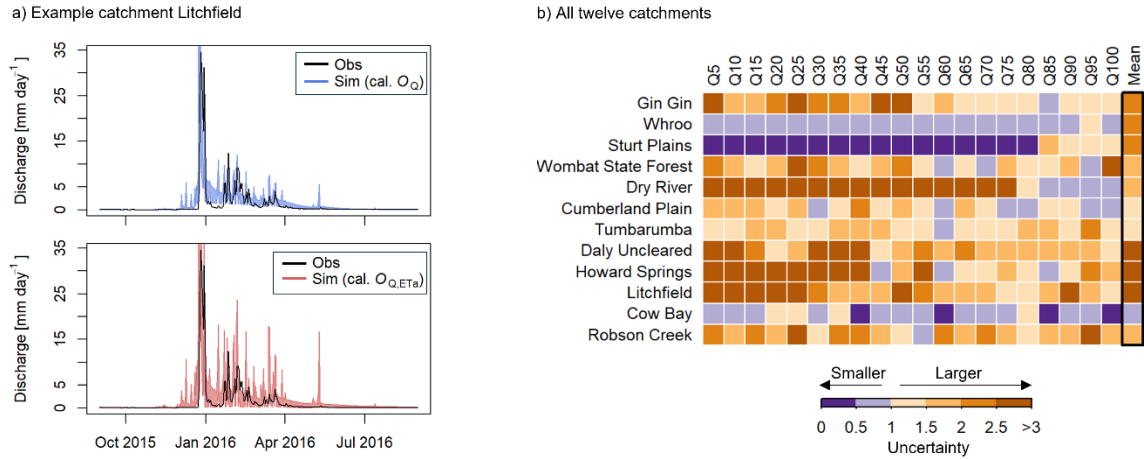


Figure S10. Repeat of Fig. 4 from the main paper, but using *field-based* actual evapotranspiration ($D_{ETa,Field}$) rather than remotely sensed information. The figure shows hydrograph uncertainty when calibrating the model with discharge (O_Q) or discharge and actual evapotranspiration ($O_{Q,ETa}$). (a) Observed and simulated hydrograph for the Litchfield catchment in a year with close to average mean annual discharge. The range in hydrograph simulations indicates the minimum and maximum value of all 100 best simulations in terms of O_Q and $O_{Q,ETa}$. (b) Change in uncertainty of the simulated hydrographs at different flow quantiles (Q5 (low flow) to Q100 (high flows)). Change is defined as the ratio of the simulated range from a calibration with $O_{Q,ETa}$ to the simulated range from a calibration with O_Q . Values smaller than 1 (purple color) indicate a reduction in uncertainty when adding actual evapotranspiration to a discharge-based calibration. Values are shown for all twelve study catchments.

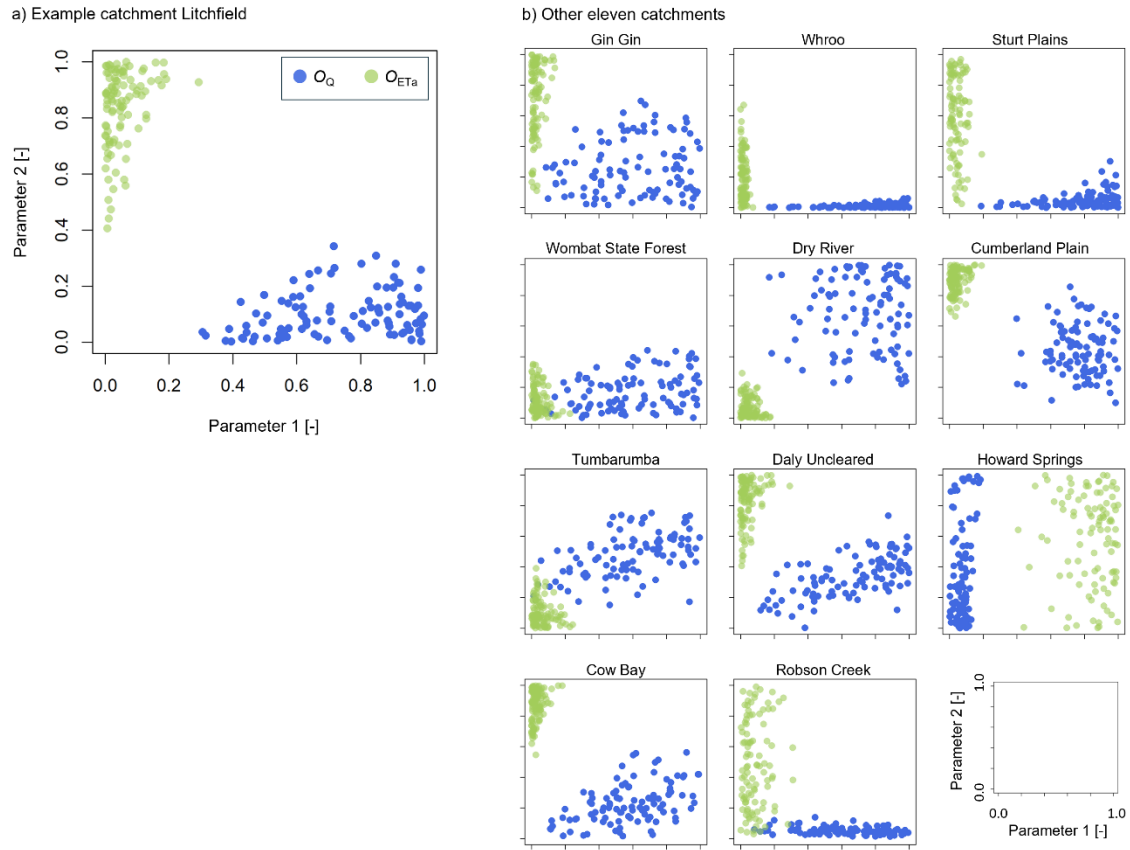


Figure S11. Repeat of Fig. 5 from the main paper, but using *field-based* actual evapotranspiration ($D_{ETa,Field}$) rather than remotely sensed information. The figure shows the parameter distribution when calibrating the model with discharge (O_Q) or actual evapotranspiration (O_{ETa}). (a) Distribution of two parameters for the 100 best parameter sets in terms of O_Q and O_{ETa} for the Litchfield catchment. In this example, parameter 1 is infiltration loss exponent [-] and parameter 2 is maximum infiltration loss [mm d^{-1}]. (b) Same as in (a) but with an example for the other eleven catchments. Note that all parameter values are normalized [0,1], and parameter 1 and parameter 2 represent different SIMHYD parameters in each case. Parameter combinations were chosen to show different separation patterns. Robson Creek is the only catchment without a point cloud separation in a two-dimensional parameter space when calibrating with O_Q and O_{ETa} .

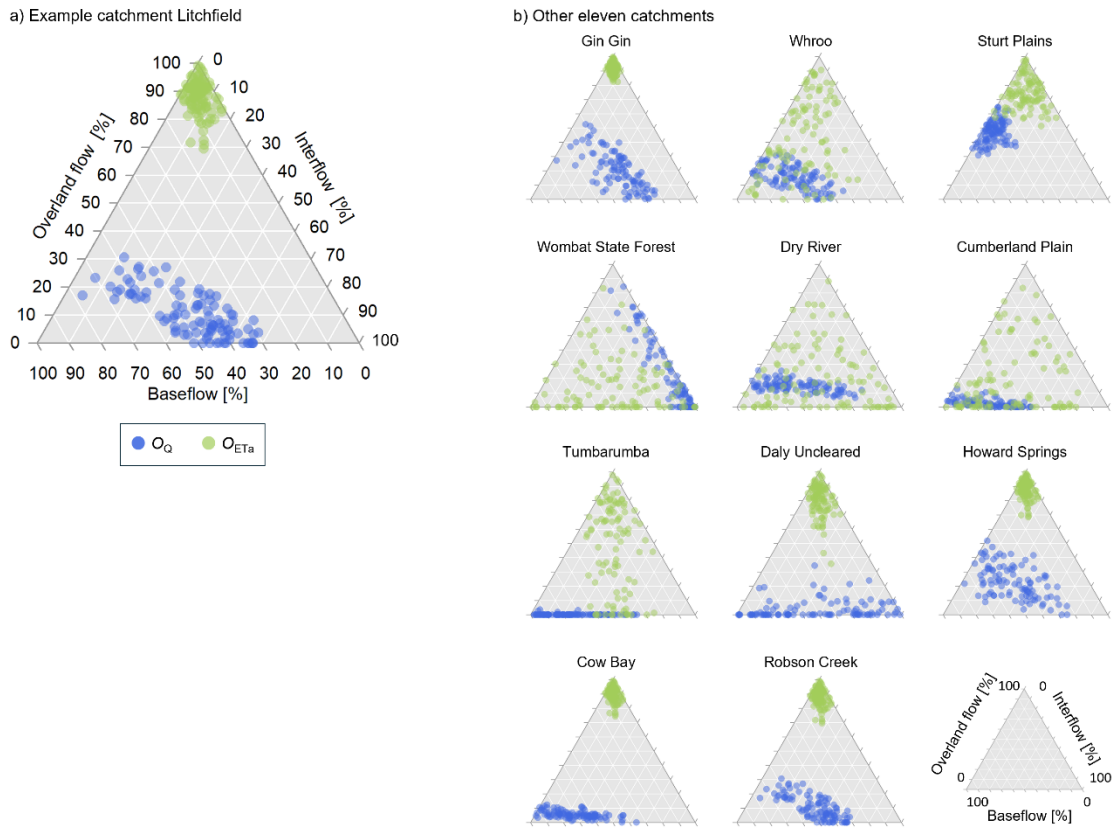


Figure S12. Repeat of Fig. 7 from the main paper, but using *field-based* actual evapotranspiration ($D_{ETa,Field}$) rather than remotely sensed information. The figure shows the flux map when calibrating the model with discharge (O_Q) or actual evapotranspiration (O_{ETa}). (a) The flux map is shown for the 100 best parameter sets in terms of O_Q and O_{ETa} for the Litchfield catchment. (b) Same as in (a) but for the other eleven catchments.

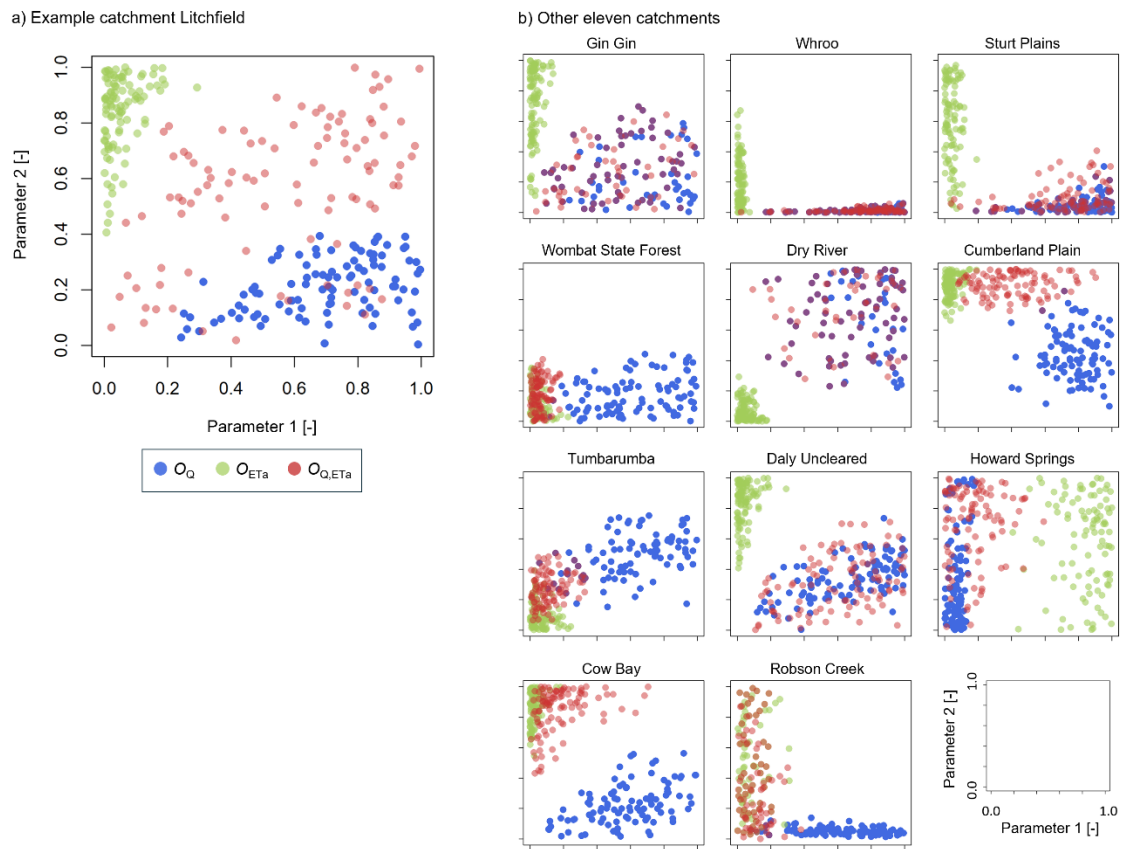


Figure S13. Repeat of Fig. S5 from the supporting information, but using *field-based* actual evapotranspiration ($O_{ETa,Field}$) rather than remotely sensed information. The figure shows the parameter distribution when calibrating the model with discharge (O_Q), actual evapotranspiration (O_{ETa}), or discharge and actual evapotranspiration ($O_{Q,ETa}$). This figure is the same as Fig. S7 with the difference that results are shown for all three calibration cases: (a) Distribution of two parameters for the 100 best parameter sets in terms of O_Q , O_{ETa} , and $O_{Q,ETa}$ for the Litchfield catchment. In this example, parameter 1 is infiltration loss exponent [-] and parameter 2 is infiltration loss [mm d^{-1}]. (b) Same as in (a) but with an example for the other eleven catchments. Note that parameter 1 and parameter 2 represent different SIMHYD parameters in each case.

Table S1. Catchment names based on the OzFlux Research and Monitoring network (providing actual evapotranspiration data) and the CAMELS-AUS v2 dataset (providing discharge data).

Catchment name based on the site names of the OzFlux Research and Monitoring network	Catchment name based on the catchment ID of the CAMELS-AUS dataset
Gin Gin	617003
Whroo	405229
Sturt Plains	G9030124
Wombat State Forest	407221
Dry River	G8140011
Cumberland Plain	212260
Tumbarumba	410061
Daly Uncleared	G8140063
Howard Springs	G8150018
Litchfield	G8150180
Cow Bay	108002A
Robson Creek	111007A